JOC The Journal of Organic Chemistry

Article

pubs.acs.org/joc

Tunable Push−Pull Interactions in 5-Nitrosopyrimidines

Eliška Procházková, Lucie Čechová, Ján Tarábek, Zlatko Janeba,* and Martin Dračínský*

Institute of Organic Chemistry and Biochemistry, Academy of Sciences of the Czech Republic, Flemingovo nam. 2, 166 10, Prague, Czech Republic

Supporting Information

ABSTRACT: The effect of push−pull interactions in a series of variously substituted 5-nitrosopyrimidines on the strength of intramolecular hydrogen bonds, the height of rotational barriers around formally single bonds, UV−vis spectra and electrochemical behavior is explored. Intramolecular charge transfer (ICT) leads to a shift of electron density from electron-donating substituents, which is readily observable by NMR spectroscopy. The 5-nitroso group is able to form strong intramolecular hydrogen bonds with neighboring amino substituents. As a result, two rotamers with reversed orientation of the 5-nitroso group are observed for compounds with two different hydrogen-bond donors in neighboring positions. The barriers of interconversion between the two rotamers are strongly influenced by ICT, whereas the ratio of such rotamers depends primarily on the character of the hydrogen-bond donors. The ICT also significantly affects the position of UV−vis absorption maxima, which can be tuned in a broad range of 100 nm by the selection of appropriate substituents. Finally, ICT influences oxidation potential of the 5-nitrosopyrimidines and the stability of the resulting nitroso radical cations, the structures of which are determined by EPR spectroscopy.

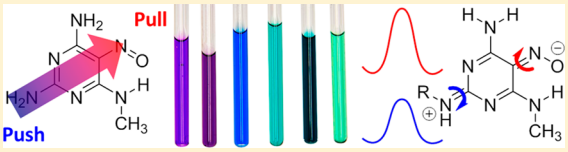

INTRODUCTION

Nitrosoarenes found many applications in synthetic organic chemistry.[1−4] They, for example, play an important role as reactive metabolites,[5−7] and are used as spin traps.[8,9] Recent studies of 5-nitrosopyrimidines revealed that the nitroso group can form unusually stable intramolecular hydrogen bonds (IMHBs) with amino substituents in neighboring C4 and C6 positions. In compounds with two different amino substituents in these positions, two rotamers of the nitroso group stabilized by the IMHBs were observed by NMR spectroscopy.[10−13] The ratio of such conformers depends significantly on the substitution of the hydrogen bond donors,[10] and the barriers of the rotamer interconversion were determined to be unusually high (>22 kcal/mol). In several cases, slow rotamer interconversion allowed the separation of pure rotamers by chromatographic techniques at room temperature. This phenomenon has been termed planamerism.[14]

One of the reasons explaining the unusual stability of these IMHBs is resonance stabilization of the hydrogen bond. High stability of intra- and intermolecular hydrogen bonds with a system of conjugated double bonds, such as in the enol form of acetylaceton, has often been observed.[15] The term resonance-assisted hydrogen bonding (RAHB) has been established for this type of hydrogen bonds, and the increased stability of these bonds was explained by a participation of distinct resonance structures differing in the position of the hydrogen atom.[16] Planar aromatic nitrosoamines can be also stabilized by RAHB.[17] We have recently investigated the resonance-assisted stabilization of IMHBs in polysubstituted 5-nitrosopyrimidines by means of a combination of NMR experiments and path integral molecular dynamics simulations that include nuclear quantum effects (NQEs).[18] It was shown that resonance stabilization of hydrogen bonds is related with the NQEs, particularly delocalization of the hydrogen atom. The formation of IMHB in 5-nitrosopyrimidines leads to elongation of formally multiple bonds and the N−H bond, and shortening of single bonds and the H···O contact.

Another principle that may contribute to the strength of the IMHBs in 5-nitrosopyrimidines is the push−pull interaction of the substituents on the pyrimidine moiety. Molecular π-systems with an electron donating (D) and an electron accepting (A) substituents are known as push−pull systems or systems with intramolecular charge transfer (ICT).[19] Push−pull interaction of such substituents has been described to be crucial, e.g., for nonlinear optical properties,[20−23] high power conversion efficiency in dye-sensitized solar cells,[24−26] electro-optic[27] and piezochromic[28] materials and supramolecular chemistry applications.[29] The use of π-excessive or π-deficient heteroaromatics as the π linker in the D-π−A systems has been shown to result in an increased ICT while the chemical and photochemical stability of these systems has been preserved.[30−32] Furthermore, the use of substituted heteroaromatic systems as the π-linker allows finer tuning of the desired electronic and optical properties.[33,34]

In all cases, where the high rotational barrier of the 5-nitroso group has been observed, three electron-donating substituents were attached to the pyrimidine skeleton together with the electron-withdrawing nitroso group. This push−pull interaction may result in a shift of electron density from the electron donors to the 5-nitroso group leading to an increase of the bond order between the substituents and pyrimidine ring (Figure 1). Both the partially double bond C5−NO and higher electron density at the nitroso group, making it a better

Received: February 29, 2016
Published: March 30, 2016

DOI: 10.1021/acs.joc.6b00446
J. Org. Chem. 2016, 81, 3780−3789

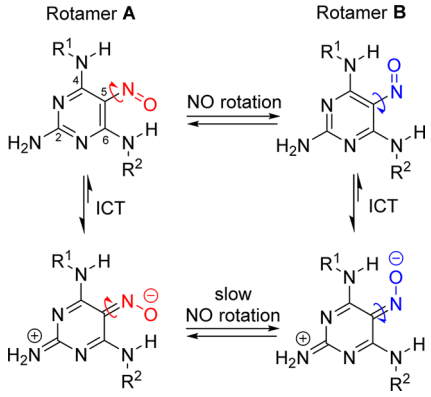

Figure 1. Push−pull interaction leading to intramolecular charge transfer (ICT) and higher rotational barriers in polysubstituted 5-nitrosopyrimidines.

hydrogen bond acceptor, may contribute to the unusually high values of the rotational barrier of the 5-nitroso group.

Herein, we investigate the effect of the push−pull interactions on the extraordinary stability of the intramolecular hydrogen bonds in polysubstituted 5-nitrosopyrimidines, which allowed, in several cases, the separation of two rotamers differing in the nitroso group orientation only.[14] For a series of newly prepared compounds (Figure 2), we determined the effects of ICT on the barriers of rotation around formally single bonds, on their UV−vis spectra, on electrochemical reactivity and stability of the generated nitroso radical cations.

RESULTS AND DISCUSSION

Synthesis. In order to study the influence of the C2 substitution on the physicochemical properties of polysubstituted 5-nitrosopyrimidines, series of pyrimidines bearing a variety of substituents (H, CH_3, $NHCH_3$, NH_2, OCH_3 and SCH_3) in C2 position has been prepared. A nucleophilic aromatic substitution (S_NAr) represents the key reaction for the modifications of the pyrimidine moiety in C2, C4 and C6 positions. Chlorine atom is usually easily replaced by the corresponding nucleophiles (e.g., amines), as well as a methoxy group that is activated toward S_NAr by the presence of strongly electron withdrawing nitroso group in C5 position. The synthesis of all pyrimidine derivatives under study is depicted in Scheme 1. Microwave-assisted (MW-assisted) synthesis is utilized where possible, as this methodology usually gives excellent yields of products in short reaction times.

Compound **1** was prepared by microwave assisted (MW-assisted) treatment of commercially available 4,6-dimethoxy-2-(methylsulfonyl)pyrimidine (**6**) with ethanolic methylamine. Nitrosation of compound **1** with isoamyl nitrite (IAN) in DMSO provided 5-nitroso derivative **2** and subsequent replacement of one of the methoxy groups with ammonia gave derivative **4b**. The treatment of starting pyrimidine **7** with IAN in DMSO at room temperature yielded 5-nitroso

Scheme 1. Synthesis of the Studied Compounds[a]

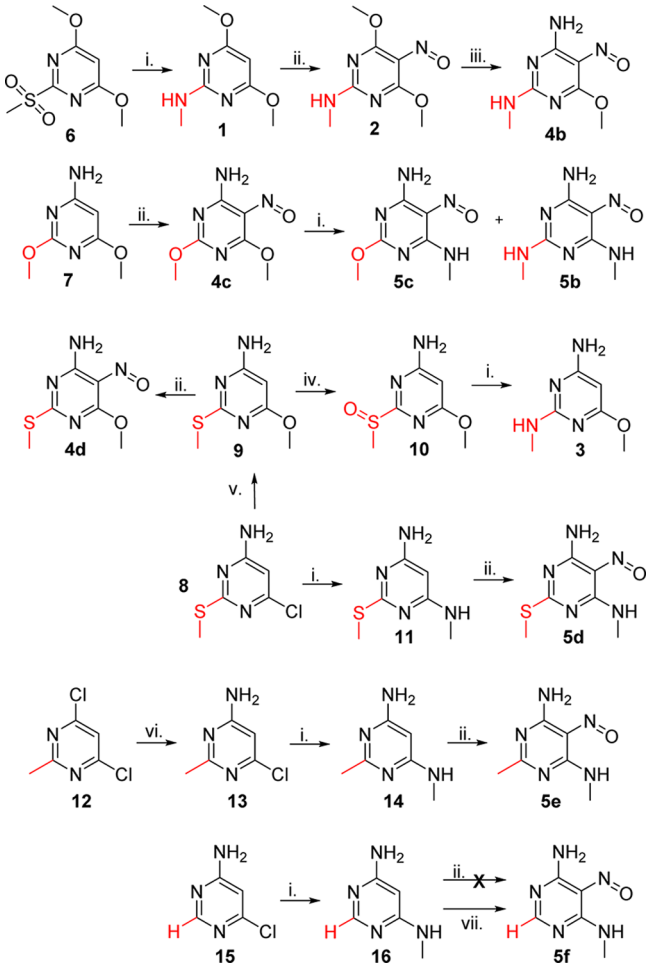

[a]Conditions: (i) methylamine (33% ethanolic solution), MW; (ii) IAN, DMSO, rt; (iii) ammonia (25% aqueous solution), rt; (iv) mPCBA, CH_2Cl_2, 0 °C; (v) MeONa, MeOH, reflux; (vi) ammonia (2.5 M ethanolic solution), MW; (vii) $NaNO_2$, HCl, H_2O, 0 °C.

derivative **4c** and subsequent MW-assisted treatment with ethanolic methylamine afforded both 2,6-di(methylamino) and 6-methylamino substituted products **5b** (60%) and **5c** (22%), respectively. Methanolysis of compound **8** gave derivative **9**, that was further nitrosylated to the final product **4d**. Furthermore, the 2-methylsulfonyl group of compound **9** was oxidized with mCPBA in dichloromethane to give 2-methylsulfinyl derivative **10**. The good leaving 2-methylsulfinyl group in derivative **10** was then replaced with methylamine to give product **3**. MW-assisted aminolysis of pyrimidine derivative **8** with ethanolic methylamine (to give intermediate **11**) followed by the treatment with IAN in DMSO led to 5-nitrosoderivative **5d**. Analogous MW-assisted ammonolysis of 4,6-dichloro-2-methylpyrimidine (**12**) with ethanolic solution

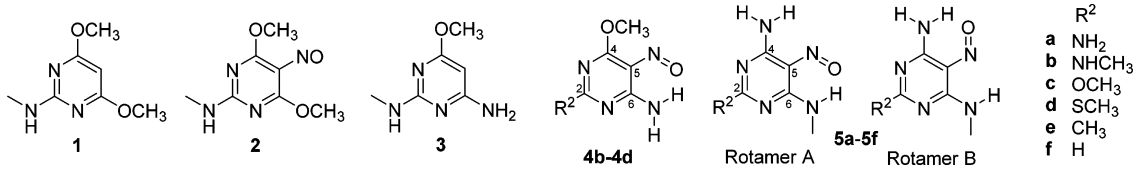

Figure 2. Chemical structures of the studied compounds.

DOI: 10.1021/acs.joc.6b00446
J. Org. Chem. 2016, 81, 3780−3789

of ammonia gave compound **13**, that was further converted to final derivative **5e** by MW-assisted treatment with ethanolic methylamine (to give intermediate **14**) and subsequent nitrosation using IAN in DMSO at room temperature. Finally, 4-amino-6-chloropyrimidine (**15**) was converted to the 5-nitrosopyrimidine derivative **5f** by a replacement of the 6-chloro group with ethanolic solution of methylamine under microwave irradiation (to give intermediate **16**) and subsequent nitrosation using $NaNO_2$ and aq. HCl (application of IAN in DMSO did not afford the desired product in this case).

NMR Spectroscopy. The presence of intramolecular charge transfer (ICT) can be inferred from chemical shift changes upon nitrosation of compound **1** as shown in Figure 3.

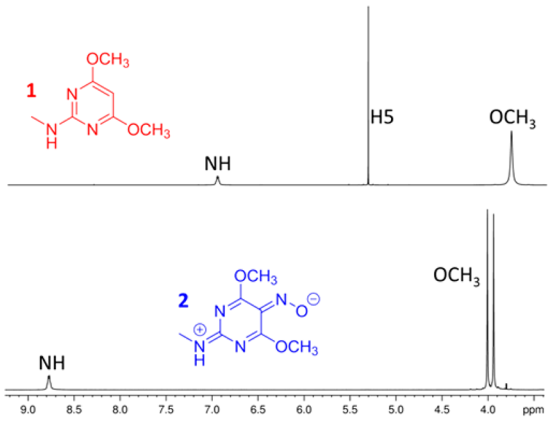

Figure 3. Part of ^{1}H NMR spectrum of compounds **1** and **2** with signal assignment.

The presence of the nitroso group in compound **2** leads to a significant deshielding of the NH hydrogen in position C2 (by 1.8 ppm), which can be explained by a partial positive charge on the nitrogen atom stabilized by the ICT. ^{15}N NMR chemical shifts of the $NHCH_3$ nitrogen (detected indirectly by H,N-HMBC experiment) also indicate large deshielding (by 25 ppm) of the methylamino group after nitrosation. The experimental changes of chemical shifts of compound **1** upon nitrosation to give derivative **2** correlate well with DFT predictions, which further confirms the ICT (details in the Supporting Information).

Furthermore, the ICT increases the C5−NO and C2−NH bond order leading to higher rotational barriers and hence to slower rotation around these bonds. The barriers of rotation around partially double bonds determined by dynamic NMR spectroscopy (dNMR) have been used as an experimental measure of the push−pull interaction.[35,36] The OCH_3 groups in compound **1** are equivalent, because the fast rotation of the $NHCH_3$ group averages their signals. On the other hand, the rotations around C5−NO or C2−NH bond are slowed down in compound **2** leading to observation of two nonequivalent signals of the methoxy groups at room temperature. When ^{1}H NMR spectrum of compound **2** is acquired at −50 °C, rotations around both the C2−NH and C5−NO bonds become slow and four signals of OCH_3 groups are observed. These four signals correspond to two nonequivalent methoxy groups in two possible conformers of the compound (*syn* and *anti* orientation of the NO and $NHCH_3$ groups). The observation of two signals of OCH_3 groups in compound **2** at room temperature can thus be caused by high rotational barrier either of C2−NH or C5−NO bond avoiding chemical shift averaging. By applying methods of dNMR at a broad temperature range (−50 to +140 °C), we determined the two rotational barriers to be 21 and 9 kcal/mol, respectively (Tables 1 and 2). The very good correlation with calculated rotational barriers allowed us to assign unambiguously the higher barrier to the C2−NH rotation.

Table 1. Observed Composition of Conformational Mixtures Resulting from Restricted Rotation around the C2−R^2 Bond, and Observed and DFT-Calculated Barriers of Rotation (kcal/mol) around the Bond

compound	R^2	R^5	$\%C_{exp}$ [a]	$\Delta G^{\ddagger}_{exp}$	$\Delta G^{\ddagger}_{calcd}$
1	$NHCH_3$	H	50[b]	14.4 ± 1.0	15.5
2	$NHCH_3$	NO	50	20.8 ± 1.0	20.4
3	$NHCH_3$	H	42 ± 2	12.8 ± 1.0	14.8
4b	$NHCH_3$	NO	30 ± 2	19.3 ± 1.0	20.1
4c	OCH_3	NO	−[c]	−[c]	8.3
4d	SCH_3	NO	−[c]	−[c]	9.2
5b	$NHCH_3$	NO	47 ± 2	19.6 ± 1.0	19.4
5c	OCH_3	NO	−[c]	−[c]	8.2
5d	SCH_3	NO	−[c]	−[c]	8.7

[a]The percentage of the rotamer with the methyl group of the C2 substituent heading toward C4 (see Figure S2 in SI). [b]The rotation around C2−$NHCH_3$ bond leads to identical structure. [c]No signal splitting due to restricted rotation around C2−R^2 bond observed at −50 °C.

Table 2. Observed Composition of Conformational Mixtures Resulting from Restricted Rotation around the C5−NO bond, and Observed and DFT-Calculated Barriers of Rotation (kcal/mol) around the Bond

compound	R^2	$\%A_{exp}$ [a]	$\Delta G^{\ddagger}_{exp}$	$\Delta G^{\ddagger}_{calcd}$(A → B)
2	$NHCH_3$	–	~9[b]	14.7
5a	NH_2	64 ± 2	23.0 ± 0.2[c]	28.6
5b	$NHCH_3$	63 ± 2	−[d]	28.5
5c	OCH_3	66 ± 2	22.0 ± 1.0	26.2
5d	SCH_3	66 ± 2	18.2 ± 1.0	25.0
5e	CH_3	66 ± 2	−[d]	24.8
5f	H	66 ± 2	16.1 ± 1.0	23.4

[a]The percentage of the rotamer with the NO group heading toward C6 (see Figure 1). [b]The height of the barrier is estimated from ^{1}H NMR spectra acquired at two temperatures only due to severe signal overlap at other temperatures. [c]The rotational barrier was determined by following the interconversion of the rotamers after dissolution of initially pure rotamer B (Figure S3 in SI). [d]Impossible to determine due to severe signal overlap.

In compounds **4b**, **4c** and **4d**, the nitroso-group oxygen atom and one of the neighboring amino NH hydrogens form an intramolecular hydrogen bond, whose presence was clearly confirmed by ^{1}H NMR spectra, where one of the amino hydrogens was shifted by 1−2 ppm to higher chemical shift values due to the deshielding caused by the hydrogen bonding. The intramolecular hydrogen bond also prevents the rotation of the 5-nitroso group as confirmed by DFT calculations, where the energy of the conformer of compound **4b** without H-bond has higher energy by 4.0 kcal/mol.

Two sets of signals in 7:3 ratio corresponding to two possible orientations of the $NHCH_3$ group in compound **4b** can be observed in proton and carbon NMR spectra and the barrier of their interconversion was determined by dNMR to be 19.3 kcal/mol (Table 1). The signals were assigned to individual

DOI: 10.1021/acs.joc.6b00446
J. Org. Chem. 2016, 81, 3780−3789

conformers on the basis of long-range heteronuclear constants (details in SI). No signal splitting into two sets was observed in NMR spectra of compounds **4c** and **4d**; only minor line broadening of proton signals was observed at −50 °C, which indicates that the C2−R^2 (R^2 = OCH_3 or SCH_3) rotational barriers are significantly lower in these compounds than in compound **4b**, where larger ICT is promoted by strongly electron-donating methylamino group in C2 position.

A comparison of the rotational barriers in compounds **3** and **4b** reveals similar difference of ca. 6.5 kcal/mol as in the case of compounds **1** and **2** but the barriers are slightly lower for the 6-amino substituted compounds **3** and **4b**.

In the case of compounds **5a**−**5f**, two IMHBs with different orientation of the 5-nitroso group are possible(Figure 1). The observed ratio of the two conformers with different orientation of the nitroso group is almost independent of the nature of the substituent in C2 position (Table 2). This observation is in clear contrast to the influence of substituents in position C4 and C6, which have been found to enable fine-tuning of the NO group rotamer ratio in a very broad range.[10] The electronic structure of compounds **5a**−**5f** is also reflected in the observed chemical shifts. The chemical shift of the 6-methylamino group hydrogen atom involved in the hydrogen bonding in rotamer A is above 11 ppm, whereas the chemical shift of the unbound hydrogen in rotamer B is in the range of 8.6−9.6 ppm (Table S2). Electron-donating substituents in position C2 increase the shielding of carbon atom C5, leading to lower chemical shift of C5. Chemical shift of carbon atom C4 in rotamer A is almost unaffected by the nature of the C2 substituent, while chemical shift of C6 increases with more electron-donating character of the substituent in the C2 position. This observation is somewhat unexpected, since electron-donating substituents normally increase shielding of carbon atoms in (hetero)-aromatic systems. However, carbon C6 in rotamer A of compounds **5a**−**5f** is directly attached to the nitrogen atom involved in the IMHB with the 5-nitroso group, and electron-donating substituents in the C2 position induce larger ICT. This leads to larger negative charge of the NO oxygen making it a better hydrogen-bond acceptor, which in turn leads to a deshielding of carbon C6. More detailed discussion of chemical shifts of compounds **5a**−**5f** is presented in SI.

The two rotamers of compound **5a** were separated by column chromatography and kinetics of the rotamer interconversion was observed by continuous measurement of ^{1}H NMR spectra of a solution of one initially pure rotamer. The barrier of rotamer interconversion was determined to be 23 kcal/mol (see details in SI).

In compound **5b** both rotational barriers around C2−$NHCH_3$ and C5−NO bonds are high enough to permit observation of four sets of signals corresponding to four possible conformers of the compound in DMSO solution at room temperature. The assignment of all NMR signals was possible thanks to NMR measurements on an 850 MHz spectrometer, where the overcrowded aliphatic region could be resolved (Figure S4), and was again based on the observation of long-range heteronuclear interactions. Analysis of variable-temperature NMR spectra allowed estimating the rotational barrier around the C2−$NHCH_3$ bond to be 19.6 kcal/mol.

In NMR spectra of compounds **5c**−**5f**, only two sets of signals were observed, which correspond to two rotamers defined by the orientation of the 5-nitroso group. No signal splitting due to slow rotation around the C2−R^2 bonds (where R^2 = OCH_3, SCH_3, CH_3, or H) was observed down to −50 °C.

The influence of protonation on the rotational barriers and rotamer ratio was determined by adding one equivalent of hydrochloric acid to the samples of compounds **4b** and **5c**. The protonation disturbs the ICT by decreasing the electron density in the pyrimidine ring. The ratio of conformers resulting from rotation of both the C2 and C5 substituents was not altered by the protonation, while both rotational barriers decreased slightly: by 0.2 kcal/mol (C2−$NHCH_3$ barrier in **4b**) and 2.0 kcal/mol (C5−NO barrier in **5c**).

The rotational barriers around the C2−R^2 and C5−NO bonds were also calculated by DFT method. A transition state (TS) with the C2 or C5 substituent in perpendicular orientation with respect to the pyrimidine ring was found in all cases and the calculated barriers agree well with experiments, although the C5−NO barriers are systematically overestimated by ca. 5 kcal/mol. This overestimation is probably due to an insufficient description of solvent effects by the polarizable continuum model (PCM) used in the calculations. Hydrogen bonding between the "naked" amino hydrogen and solvent molecules will stabilize the transition state, but these specific interactions are not modeled well with the PCM approach.[37] Generally, electron-donating substituents in position 2 increase both rotational barriers. The absence of the nitroso group in C5 position leads to a drop of the C2−R^2 barrier by 5 kcal/mol (compounds **1** and **2**, and **3** and **4b**, Table 1), and the change from strongly electron-donating amino and methylamino groups to less electron-donating substituents leads to a significant decrease of the C2−R^2 barrier. The presence of the intramolecular hydrogen bond between NO and adjacent NH groups stabilizes the planar arrangement of the compounds making the C5−NO rotational barrier significantly higher and the barrier in compounds **5a**−**5f** varies in a broad range depending on the nature of the C2 substituent.

The ICT is also reflected in bond lengths and dipole moments of the molecules. In the TS structures, where efficient ICT is blocked by the nonplanar arrangement of the molecules, the C5−N and N═O bond lengths are almost constant for all molecules **5a**−**5f** and the calculated dipole moment varies only slightly. On the other hand, in the energy-minima structures, the C5−N bond is by more than 0.1 Å shorter and the N═O bond by 0.05 Å longer than in the TS structures. Furthermore, both distances and the dipole moments are significantly substituent dependent (Table S3 in the SI); more electron-donating substituents in C2 position make the C5−N bond shorter, the N═O bond longer and the dipole moment larger. Similarly, the C2−$NHCH_3$ bond is significantly shorter in compound **2** (with NO group in position 5) than in compound **1**.

UV−Vis Absorption Spectra. The UV−vis spectra of the 5-nitrosopyrimidines solutions in DMSO exhibit one weak electronic transition in the visible region (552−644 nm, Figure 4) and one strong transition in the UV region (336−358 nm, Figure S7), which could be assigned with the help of time-dependent density-functional theory (TD-DFT) calculations. The color of the solutions ranging from violet to green (Figure S8) is caused by the weak electronic transition between lone pair and antibonding π orbitals (n → π^*, HOMO → LUMO), and the UV band is caused by $\pi \rightarrow \pi^*$ (HOMO−2 → LUMO) transition. The position of the maximum in the visible region depends significantly on the substituent in C2 position (Table 3, Figure 4) with a large hypsochromic shift (more than 100 nm) for electron-donating substituents. On the other hand, the position of the UV maximum is significantly less substituent-

DOI: 10.1021/acs.joc.6b00446
J. Org. Chem. 2016, 81, 3780−3789

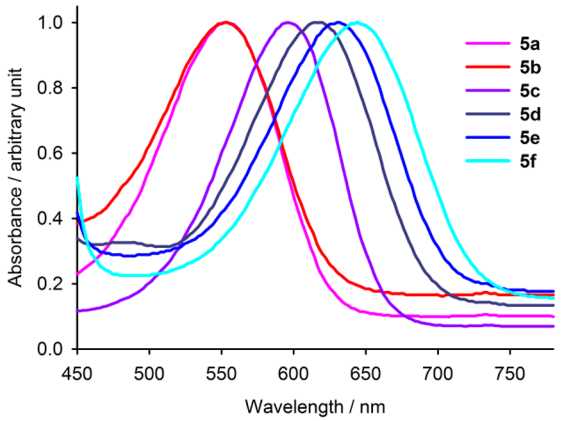

Figure 4. Normalized absorption spectra of compounds **5a**–**5f** in the visible region of light.

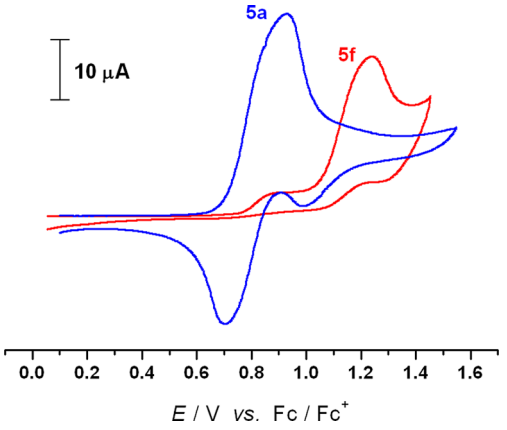

Figure 5. Cyclic voltammograms of compounds **5a** and **5f** in 0.25 M $TBAPF_6/CH_3CN$. Half-peak potential ($E_{p/2}$) of the first anodic wave is 0.787 and 1.111 V for **5a** and **5f**, respectively. The potential scale is referenced against that of the Fc/Fc^+ redox couple. The scan rate was 5 mV/s.

dependent. Electron-donating substituents in C2 position increase the energy of both frontier orbitals. The effect is bigger, however, for LUMO, which results in an increase of the energy gap between HOMO and LUMO for stronger electron-donors (Table 3).

EPR Spectroelectrochemistry. The push–pull effect leads to an increase of the electron density in the 5-nitroso group and can, therefore, lead to its easier oxidation. We performed a series of EPR spectroelectrochemical experiments in order to corroborate the influence of the push–pull effect on the NO oxidation and to confirm the structure of oxidized species.

Figure 5 shows cyclic voltammograms of compounds **5a** and **5f**. The most remarkable feature, related to the ease of oxidation, is the potential difference of the first anodic wave between compounds **5f** and **5a** ($\Delta E_{p/2,ox} = E_{p/2,ox}(\mathbf{5f}) - E_{p/2,ox}(\mathbf{5a}) = 0.32$ V). While the cyclic voltammogram of **5a** is quasi-reversible, that of **5f** is completely irreversible, probably due to a follow-up chemical reaction of the **5f** radical cation (see the EPR analysis below). Therefore, the half-peak potential values ($E_{p/2}$) are compared instead of the more common half-wave potentials ($E_{1/2}$).[38,21] Half-wave potentials, which are directly related to standard redox potentials, can be estimated only from voltammograms showing a fully reversible electron transfer.[38] As demonstrated by NMR spectroscopy, both 5-nitroso-group rotamers (A and B) of compounds **5a** and **5f** exist in solution. DFT calculations revealed that the oxidation potential difference between rotamer A and B is 0.013 and 0.018 V for compounds **5a** and **5f**, respectively. These small differences cannot be observed in the voltammograms, but may contribute to their rather broad shape. The oxidation potential difference between compounds **5f** and **5a** obtained by DFT (0.290 V for rotamer A and 0.260 V for rotamer B) are reasonably close to the experimental $\Delta E_{p/2,ox}$ values. Moreover, the potential difference between **5f** and **5a** in the moment of observation of the first EPR spectrum during the EPR spectroelectrochemical experiment was 0.37 V, which also correlates well with the $\Delta E_{p/2,ox}$.

The assumption that the anodic waves correspond to one-electron oxidation from neutral to radical cationic species was proved by EPR spectroscopy measured simultaneously during the cyclovoltammetric scan. Figure 6 shows representative EPR

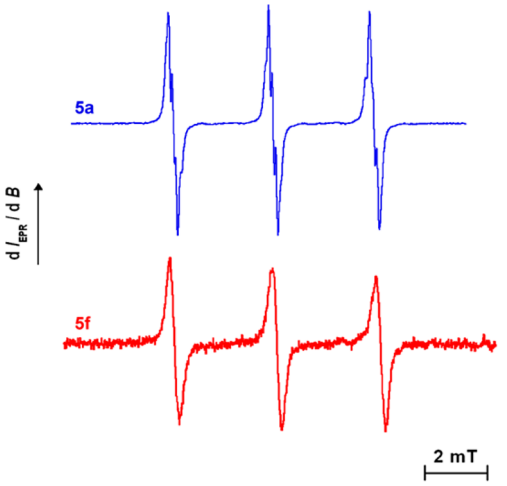

Figure 6. Representative EPR spectra recorded during the EPR spectroelectrochemical experiments in 0.25 M $TBAPF_6$/ACN solution of compounds **5a** and **5f**. The starting concentration of individual compounds in electrolyte solution was 2 mM. Corresponding DFT calculated spin densities are shown in SI.

Table 3. Observed and Calculated Wavelengths of UV–Vis Absorption Maxima (nm) and Calculated Energies of Frontier Orbitals (eV) of Compounds 5a–5f

compound	R^2	UV_{EXP}	VIS_{EXP}	UV_{CALC}	VIS_{CALC}	HOMO	LUMO
5a	NH_2	336	552	321	570	−0.224	−0.089
5b	$NHCH_3$	340	552	326	567	−0.223	−0.088
5c	OCH_3	342	596	330	597	−0.230	−0.097
5d	SCH_3	354	618	347	617	−0.231	−0.102
5e	CH_3	354	630	348	627	−0.231	−0.103
5f	H	358	644	350	642	−0.234	−0.107

DOI: 10.1021/acs.joc.6b00446
J. Org. Chem. 2016, 81, 3780–3789

spectra recorded in situ during the electrochemical oxidation of compounds **5a** and **5f**. The spectra exhibit large hyperfine splitting ($a_{iso} \approx 3.1$ mT) between three equally intensive lines. Large a_{iso} values can be attributed to nitroso radical cations (—N═O$^{\bullet+}$) rather than neutral nitroxyl (>N—O$^{\bullet}$) radicals,[39] which was also confirmed by DFT calculations, where an excellent agreement of calculated EPR parameters of the radical cations with experiment was found (see SI). Super-hyperfine splitting (SHFS) can be well recognized in the EPR spectrum of oxidized compound **5a**. By comparison with spectra of similar compounds and with DFT calculations (see SI), we conclude that the SHFS is caused by interactions of the unpaired electron with the amino groups in the neighboring positions C4 and C6. The expected SHFS from the amino groups in the spectrum of oxidized compound **5f** was not observable because the radical cation of **5f** was not persistent enough during the experiment, which leads to broader EPR lines. After the oxidation of **5f** the EPR signal appears but it rapidly decreases during the rereduction. This observation is consistent with the irreversible voltammogram of **5f**. On the other hand, the signal appearance and disappearance was completely reversible during the oxidation and rereduction process for compound **5a** and other 5-nitrosopyrimidines with amino substituent in C2 position (shown in SI). Therefore, the "push−pull" effect may also play an important role in the stabilization of the 5-nitrosopyrimidine radical cations.

As shown by NMR spectroscopy, two stable conformers (rotamer A and B) are present in solutions of compounds **5a**−**5f** and therefore, the presented voltammograms and EPR spectra correspond to the mixture of both as well. However, DFT calculations (shown in the SI) revealed that hyperfine splitting/coupling as well as *g*-factors of both rotamers of compounds **5a** and **5f** are very close to each other. This complicates the analysis of SHFS by simulations of the EPR spectra of these compounds. Therefore, we also performed low-temperature EPR spectroelectrochemical experiments with pure rotamer A of another 5-nitrosopyrimidine derivative (depicted in SI) that was shown recently to be easily isolable and sufficiently stable.[14] The resulting EPR spectrum corresponding to pure rotamer A of the radical cation was then readily analyzed by spectral simulations and all spectral parameters including SFHS values were determined (see details in SI).

CONCLUSIONS

We have demonstrated that the "push−pull" effect, based on cooperative interactions of the electron-accepting 5-nitroso group and electron-donating substituents in other positions of the pyrimidine moiety, has a large impact on electronic structure in polysubstituted 5-nitrosopyrimidines. This effect is detectable in NMR spectra by significant chemical shift changes and by a dramatic increase of rotational barriers around formally single bonds. The presence of a single electron-accepting nitroso group increased the rotational barrier of $NHCH_3$ group in C2 position by 6.5 kcal/mol leading to observation of two sets of signals in NMR spectra at room temperature corresponding to two possible rotamers of the methylamino group. Similarly, the electron-donating character of the C2 substituent has an influence on the C5−NO bond order leading to large changes of the rotational barriers around this bond.

The intramolecular charge transfer (ICT) also contributes significantly to the stabilization of intramolecular hydrogen bonds in 5-nitrosopyrimidines. In compounds with two competing intramolecular hydrogen bonds, ICT significantly affects the interconversion barrier between the two structures but not the composition of the equilibrium mixture. Both the partially double C5−NO bond and higher electron density at the nitroso oxygen, making it a better hydrogen bond acceptor, may contribute to the height of the rotational barrier of the 5-nitroso group. As shown previously, the composition of the equilibrium mixture (the rotamer ratio) is, on the other hand, strongly influenced by the nature of the hydrogen bond donors. A clever design of 5-nitrosopyrimidines can thus lead to development of versatile "molecular switches" with tunable equilibrium composition and interconversion ("switching") barrier.

The ICT also influences the reactivity of 5-nitrosopyrimidines, namely the oxidation of the nitroso group to nitroso radical cation. Electron donors attached to the pyrimidine ring increase the electron density of the nitroso group, which is then oxidized more easily.

Polysubstituted 5-nitrosopyrimidines may find various interesting applications. For example, 5-nitrosopyrimidines with intramolecular hydrogen bond forming a pseudoring have been proposed to behave as purine mimics with potential use in drug development. Furthermore, these colorful compounds also absorb strongly in the UV region of light, which makes them promising candidates for (bio)sensing. For that purpose, the position of absorption maxima can be finely tuned by choice of appropriate substituents.

EXPERIMENTAL SECTION

General Instrumentation and Calculations. Starting compounds **6**, **7**, **8**, **12**, and **15** (Scheme 1) and other chemicals were purchased from commercial suppliers. Solvents were dried by standard procedures. Unless otherwise stated, solvents were evaporated at 40 °C/2 kPa, and the compounds were dried over P_2O_5 at 2 kPa. Analytical TLC was performed on silica gel precoated aluminum plates with fluorescent indicator. Spots were visualized with UV light (254 nm). Column chromatography was carried out on silica gel (40−63 μm). Mass spectra were measured on a Q-Tof micro and HR MS were taken on a LTQ Orbitrap XL spectrometer. Melting points were determined on a Stuart SMP3Melting Point Apparatus and are uncorrected.

The microwave-assisted reactions were carried out in CEM Discover (Explorer) microwave apparatus, 24-position system for 10 mL vessels sealed with Teflon septum. It was operated at a frequency of 2.45 GHz with continuous irradiation power from 0 to 300 W. The solutions were steadily stirred during the reaction. The temperature was measured with an IR sensor on the outer of the process vessel. The vials were cooled to ambient temperature with gas jet cooling system. The pressure was measured with an inboard CEM Explorer pressure control system (0−21 bar).

The NMR spectra for structure determination were recorded at room temperature on a spectrometer operating at 850.3 MHz for ^{1}H and 213.8 MHz for ^{13}C, or at 500.0 MHz for ^{1}H and 125.7 MHz for ^{13}C, or at 401.0 MHz for ^{1}H and 100.8 MHz for ^{13}C in DMSO-d_6 solutions (referenced to the solvent signal δ = 2.50 and 39.70 ppm, respectively). 1D and 2D correlation NMR experiments (COSY, HSQC, HMBC) were combined for the signal assignment. The variable-temperature NMR spectra were recorded on a spectrometer operating at 499.9 MHz for ^{1}H in DMSO-d_6 or DMF-d_6 solutions.

The barriers of rotation around C5−N and C2−R^2 bonds were determined by complete line-shape analysis of variable-temperature ^{1}H NMR spectra (dNMR approach). Where possible, the analysis was done for singlet signals of nonexchangeable protons (OCH_3, CH_3 groups), because chemical exchange of NH hydrogen atoms with traces of water present in the solutions complicates the analysis of the

DOI: 10.1021/acs.joc.6b00446
J. Org. Chem. 2016, 81, 3780−3789

line-shapes of signals of these protons and of the protons coupled with these protons ($NHCH_3$ groups). Note, however, that the signals were sometimes overlapped with water or solvent residual signals leading to a limited number of available temperature points for the analysis. Therefore, the error bars were estimated to be higher than usually found in dNMR analysis. The influence of protonation on the rotational barriers was studied on DMSO-d_6 solutions of compounds **4b** and **5c** with one equivalent of hydrochloride acid.

EPR spectra were measured on EMX^{plus}−10/12 CW (continuous wave) EPR spectrometer equipped with the *Premium X*-band microwave bridge. Flat EPR quartz cell was used during the EPR spectroelectrochemical experiments at room temperature. A home-made three-electrode system consisting of a Pt-wire contacted with Pt-μ-mesh, serving as a working electrode, a quasireference Ag-wire electrode and Pt-wire, serving as a counter electrode, was inserted into the flat cell. The nonactive electrode parts were isolated either with a Teflon tape or sealed in a glass capillary. After each EPR spectroelectrochemical measurement, stability of the Ag-quasireference electrode was checked against the ferrocene/ferrocenium (Fc/Fc^+) couple. All presented potentials are calculated against this redox couple. The solution of the studied compound in 0.25 M $TBAPF_6$/ACN was intensively flushed with N_2 gas before every experiment, in order to minimize the influence of the air oxygen on the electrochemical experiments and on the EPR line broadening. Simultaneous voltammetric/potentiostatic experiments were controlled by the Potentiostat/Galvanostat Autolab PGSTAT302N. Low voltammetric scan rate (ν = 5 mVs^{-1}) allowed the determination of every potential corresponding to the middle of the EPR spectrum ($dI_{EPR}/dB = 0$) with the precision of ±4 mV. This enabled assignment of the EPR spectra to paramagnetic species formed at defined potential. The spectroelectrochemical experiments at lower temperatures (258 K) were performed with a compatible EPR flat cell with 3-electrode system for the variable temperature setup, and temperature was controlled by the liquid/gas nitrogen unit ER 4141VT-U and the Win-EPR acquisition software. The *g*-factor of the radical ionic species was determined using a built-in spectrometer frequency counter and an ER 036TM NMR-Teslameter.

Simulation of EPR spectra was done within the *EasySpin 5.0.16* package[40,41] and treated by the *Origin* data analysis software. The modulation amplitude, central field, sweep width, microwave frequency and the spectral resolution (number of points) were included in the simulation.

The geometry of all of the studied structures was optimized at the DFT level of theory, using B3LYP functional[42,43] and a standard 6-31+G(d,p) basis set. The NMR parameters were calculated using the GIAO method with polarizable continuum model used for implicit DMSO solvation.[44,45] The Gaussian09 program package was used throughout this study.[46] The QST3 optimization method[47,48] was applied in the search for the transition state structures of the rotamer interconversion, that is the structures of the reactant, product, and estimated transition state were used as input for the TS search. The vibrational frequencies and free energies were calculated for all of the optimized structures, and the stationary-point character (a minimum or a first-order saddle point) was thus confirmed. Five lowest-energy electronic transitions for the compounds **5a**−**5f** were calculated with the time-dependent DFT method[49] with PCM method of DMSO solvation.

The EPR hyperfine coupling(A)/splitting(a) constants (HFCCs/HFSCs) as well as the g-factors and the spin densities were calculated by B3LYP using the double- and triple-ζ basis sets: EPR−II for C and H atoms, EPR−III for N and O atoms.[50] The oxidation potential of the studied nitroso pyrimidines was estimated by Born−Haber cycle,[51] evaluating the Gibbs free energies of the neutral and radical cationic species in the gas-phase and in the solution environment, with M06L local density functional[52] and augmented cc-pVTZ Dunning's basis set[53] (see details in the Supporting Information). All computations for the open-shell systems (radical cations) were performed in unrestricted fashion and the resulting spin contamination was always small with the eigenvalue of $\hat{S}^2$ not exceeding 0.77. Solvent (acetonitrile) effects in the EPR calculations were incorporated by the self-consistent reaction field theory at the level of conductor-like polarizable continuum model C-PCM.[44,45] All geometries and spin densities were visualized by *VMD* software package.[54,55]

General Procedure A. Isoamyl nitrite (IAN, 1.1 equiv) was added dropwise to the solution of starting compound (**1**, **7**, **9**, **11** and **14**) in DMSO (20−40 mL). The reaction mixture was stirred at room temperature overnight and water (20−40 mL) was added. Compound **4c** precipitated from the solution and product was filtrated of. The reaction mixtures with products **2**, **4d**, **5d** and **5e** were extracted with EtOAc (3 × 30 mL) and the products were isolated by silica gel column chromatography (10% MeOH in $CHCl_3$).

*4,6-Dimethoxy-N-methylpyrimidin-2-amine (**1**).* A mixture of **6** (400 mg, 1.8 mmol) and methylamine (61.4 mg, 2 mmol, 33% ethanolic solution) in iPrOH (20 mL) was treated under MW conditions (130 °C, 30 min). The reaction mixture was diluted with water (20 mL) and extracted with EtOAc (3 × 30 mL). The combined organic layers were dried over $MgSO_4$ and filtered. The resulting mixture was evaporated under vacuum and product was isolated by silica gel flash chromatography (5−10% MeOH in $CHCl_3$). Compound **1** (268 mg, 89%) was obtained as a white solid with mp 123−125 °C. ^{1}H NMR (500.0 MHz, DMSO-d_6) 6.98 (1H, q, J_{NH-CH3} = 4.7, NH), 5.33 (1H, s, H5), 3.78 (6H, bs, O−CH_3), 2.77 (3H, d, J_{CH3-NH} = 4.7, NH-**CH_3**); ^{13}C NMR (125.7 MHz, DMSO-d_6) 171.6 (C4 and C6), 162.2 (C2), 77.6 (C5), 53.2 (O−CH_3), 27.8 (NH−CH_3); ESI MS, m/z (%) 170.2 $[M + H]^+$; HRMS (ESI) calcd for $C_7H_{12}N_3O_2$ $[M + H]^+$ 170.0924, found 170.0922.

*4,6-Dimethoxy-N-methyl-5-nitrosopyrimidin-2-amine (**2**).* Treatment of **1** (200 mg, 1.2 mmol) with IAN (154 mg, 1.3 mmol) by general procedure A gave **2** (88 mg, 37%) as a green solid with mp 185−188 °C. ^{1}H NMR (500.0 MHz, DMSO-d_6) 8.78 (1H, q, J_{NH-CH3} = 4.7, NH), 4.01 and 3.94 (2 × 3H, 2*s*, O−CH_3), 2.93 (3H, d, J_{CH3-NH} = 4.7, NH−CH_3); ^{13}C NMR (125.7 MHz, DMSO-d_6) 161.2 (C2), 141.6 (C5), 54.3 (O−CH_3), 28.3 (NH−CH_3), C4 and C6 were not detected at r.t.; ESI MS, m/z (%) 199.2 $[M + H]^+$; HRMS (ESI) calcd for $C_7H_{11}N_4O_3$ $[M + H]^+$ 199.0825, found 199.0824.

*6-Methoxy-2-(methylthio)pyrimidin-4-amine (**9**).* A mixture of sodium methoxide (308 mg, 5.7 mmol) in MeOH (10 mL) was slowly added to the solution of **8** (300 mg, 1.7 mmol) in MeOH (30 mL). The reaction mixture was refluxed for 72 h. The solution was cooled down, diluted with water (30 mL) and extracted with EtOAc (3 × 30 mL). The organic layers were collected, dried over $MgSO_4$ and filtered. The solvent was evaporated under vacuum. Compound **9** (264 mg, 91%) was obtained as a white solid with mp 125−126 °C. ^{1}H NMR (500.0 MHz, DMSO-d_6) 6.66 (2H, bs, 4-NH_2), 5.42 (1H, s, H5), 3.77 (3H, s, O−CH_3), 2.40 (3H, s, S-CH_3); ^{13}C NMR (125.7 MHz, DMSO-d_6) 169.8 (C-2), 169.2 (C-6), 165.3 (C-4), 81.3 (C-5), 53.2 (O−CH_3), 2.40 (3H, s, S-CH_3); ESI MS, m/z (%) 172.1 $[M + H]^+$; HRMS (ESI) calcd for $C_6H_{10}N_3OS$ $[M + H]^+$ 172.0539, found 172.0536.

*6-Methoxy-2-(methylsulfinyl)pyrimidin-4-amine (**10**).* Compound **9** (200 mg, 1.2 mmol) was dissolved in DCM (40 mL) and obtained solution was cooled to 0 °C. Mixture of *m*CPBA (309 mg, 1.8 mmol) in DCM (20 mL) was then added dropwise during 30 min. After full conversion (TLC), solvent was evaporated under vacuum. Silica gel column chromatography (10% MeOH in $CHCl_3$) gave **10** (159 mg, 71%) as a white solid with mp 187−190 °C. ^{1}H NMR (401.0 MHz, DMSO-d_6) 7.18 (2H, bs, 4-NH_2), 5.71 (1H, s, H5), 3.82 (3H, s, 6-OCH_3), 2.77 (3H, s, SO−CH_3); ^{13}C NMR (100.8 MHz, DMSO-d_6) 172.5 (C2), 170.0 (C6), 166.2 (C4), 85.2 (C5), 54.0 (6-OCH_3), 39.4 (SO−CH_3); ESI MS, m/z (%) 210.1 $[M + Na]^+$; HRMS (ESI) calcd for $C_6H_{10}N_3O_2S$ $[M + H]^+$ 188.0488, found 188.0487.

*4-Methoxy-N^2-methylpyrimidin-2,6-diamine (**3**).* A mixture of **10** (100 mg, 0.5 mmol) in *i*PrOH (10 mL) was treated under MW conditions (150 °C, 60 min). Water (50 mL) was added and obtained solution was extracted with EtOAc (3 × 30 mL). Organic layers were collected, dried over $MgSO_4$ and filtered. Solvent was evaporated under vacuum. Silica gel column chromatography gave product **3** (30 mg, 39%) as a white solid with mp 148−150 °C. ^{1}H NMR (500.0 MHz, DMSO-d_6) 6.29 (1H, bs, NH), 6.06 (2H, s, 6-NH_2), 5.03 (1H,

DOI: 10.1021/acs.joc.6b00446
J. Org. Chem. 2016, 81, 3780−3789

s, H5), 3.69 (3H, s, O−CH_3), 2.70 (3H, d, J_{CH3-NH} = 4.8, NH−CH_3); ^{13}C NMR (125.7 MHz, DMSO-d_6) 170.3 (C4), 165.9 (C6), 162.7 (C2), 75.6 (C5), 52.4 (O−CH_3), 28.0 (NH−CH_3); ESI MS, m/z (%) 155.2 [M + H]$^+$; HRMS (ESI) calcd for $C_6H_{11}N_4O$ [M + H]$^+$ 155.0927, found 155.0925.

*4-Methoxy-N^2-methyl-5-nitrosopyrimidin-2,6-diamine (**4b**).* Compound **2** (100 mg, 0.5 mmol) was treated with ammonia (25% aqueous solution, 15 mL) for 1 h. Water (20 mL) was added and the obtained solution was extracted with EtOAc (3 × 15 mL). Organic layers were collected, dried over the $MgSO_4$, filtered and evaporated under vacuum. Silica gel column chromatography (10% MeOH in $CHCl_3$) gave **4b** (35 mg, 38%) as a pink solid with mp 229−231 °C (decomp.). ^{1}H NMR (401.0 MHz, DMSO-d_6) Rotamer C (see Figure S2 for the structure of the rotamers): 9.90 (1H, d, J_{GEM} = 3.5, 6-NH^A), 8.17 (1H, q, J_{NH-CH3} = 4.8, 2-NH), 7.89 (1H, d, J_{GEM} = 3.5, 6-NH^B), 4.11 (3H, s, O−CH_3), 2.93 (3H, d, J_{CH3-NH} = 4.8, NH−CH_3), Rotamer D: 10.29 (1H, d, J_{GEM} = 3.8, 6-NH^A), 8.34 (1H, q, J_{NH-CH3} = 4.9, 2-NH), 8.25 (1H, d, J_{GEM} = 3.8, 6-NH^B), 4.03 (3H, s, O−CH_3), 2.84 (3H, d, J_{CH3-NH} = 4.9, NH−CH_3); ^{13}C NMR (100.8 MHz, DMSO-d_6) Rotamer C: 171.1 (C4), 162.3 (C2), 150.7 (C6), 139.8 (C5), 54.3 (C4−OCH_3), 28.2 (NH−CH_3), Rotamer D: 170.2 (C4), 161.8 (C2), 150.7 (C6), 139.7 (C5), 54.2 (C4−OCH_3), 28.2 (NH−CH_3); ESI MS, m/z (%) 184.2 [M + H]$^+$; HRMS (ESI) calcd for $C_6H_9N_5O_2Na$ [M + Na]$^+$ 206.0648, found 206.0646.

*2,4-Dimethoxy-5-nitrosopyrimidin-6-amine (**4c**).* Treatment of **7** (300 mg, 2.0 mmol) with IAN (257 mg, 2.2 mmol) by general method A gave **4c** (220 mg, 60%) as a blue solid with mp 192−194 °C. ^{1}H NMR (500.0 MHz, DMSO-d_6) 10.08 and 8.80 (2 × 1H, 2 × bs, NH_2), 4.15 (3H, s, 4-O−CH_3), 3.93 (3H, s, 2-O−CH_3); ^{13}C NMR (125.7 MHz, DMSO-d_6) 173.3 (C4), 166.1 (C2), 149.3 (C6), 140.8 (C5), 55.6 (2-O−CH_3), 55.2 (4-O−CH_3); ESI MS, m/z (%) 185.1 [M + H]$^+$; HRMS (ESI) calcd for $C_6H_9N_4O_3$ [M + H]$^+$ 185.0669, found 185.0670.

*4-Methoxy-2-(methylthio)-5-nitrosopyrimidin-6-amine (**4d**).* Treatment of **9** (180 mg, 1.0 mmol) with IAN (129 mg, 1.1 mmol) by general method A gave **4d** (80 mg, 40%) as a green solid with mp 179−182 °C. ^{1}H NMR (500.0 MHz, DMSO-d_6) 9.95 (1H, s, NH^A), 8.72 (1H, s, NH^B), 4.17 (3H, s, O−CH_3), 2.55 (3H, s, S-CH_3); ^{13}C NMR (125.7 MHz, DMSO-d_6) 177.9 (C2), 168.3 (C4), 140.4 (C5), 55.2 (C4−O-**CH_3**), 14.1 (C2−S-**CH_3**), C6 was not detected at r.t.; ESI MS, m/z (%) 201.1 [M + H]$^+$; HRMS (ESI) calcd for $C_6H_9N_4O_2S$ [M + H]$^+$ 201.0440, found 201.0441.

Synthesis of Compounds 5b and 5c. Compound **4c** (100 mg, 0.5 mmol) was dissolved in *i*PrOH (15 mL) and 3.0 equiv of methylamine (47 mg, 1.5 mmol, 33% ethanolic solution) were added. The reaction mixture was heated under MW conditions (160 °C, 1 h). Water (30 mL) was added and the mixture was extracted with EtOAc (4 × 15 mL). Organic layers were collected, dried over $MgSO_4$ and filtered. The solvents were evaporated under vacuum. Silica gel column chromatography (10% MeOH in $CHCl_3$) gave **5c**. Water layer was evaporated under vacuum and crystallization (from MeOH) gave **5b**.

*N^2,N^6-Dimethyl-5-nitrosopyrimidin-2,4,6-triamine (**5b**).* Compound **5b** (60 mg, 65%) was obtained as a pink solid with mp >300 °C. ^{1}H NMR (850.3 MHz, DMSO-d_6) Rotamer CA (see Figure S4 for the structure of the rotamers): 11.13 (1H, q, J_{NH-CH3} = 4.8, 6-NH), 8.23 (1H, s, 4-NH^A), 7.74 (1H, q, J_{NH-CH3} = 4.8, 2-NH), 7.54 (1H, s, 4-NH^B), 2.84 (3H, d, J_{CH3-NH} = 4.8, 2-NH-**CH_3**), 2.82 (3H, d, J_{CH3-NH} = 4.8, 6-NH-**CH_3**), Rotamer CB: 10.26 (1H, d, J_{GEM} = 4.8, 4-NH^A), 8.81 (1H, q, J_{NH-CH3} = 4.7, 6-NH), 7.64−7.60 (2H, m, 4-NH^B and 2-NH), 2.98 (3H, d, J_{CH3-NH} = 4.7, 6-NH-**CH_3**), 2.88 (3H, d, J_{CH3-NH} = 4.8, 2-NH-**CH_3**), Rotamer DA: 11.47 (1H, q, J_{NH-CH3} = 4.9, 6-NH), 7.97 (1H, s, 4-NH^A), 7.66 (1H, q, J_{NH-CH3} = 4.8, 2-NH), 7.23 (1H, s, 4-NH^B), 2.89 (3H, d, J_{CH3-NH} = 4.9, 6-NH-**CH_3**), 2.84 (3H, d, J_{CH3-NH}= 4.8, 2-NH-**CH_3**), Rotamer DB: 10.64 (1H, d, J_{GEM}= 4.6, 4-NH^A), 8.58 (1H, q, J_{NH-CH3} = 4.6, 6-NH), 8.01 (1H, d, J_{GEM} = 4.6, 4-NH^B), 7.79 (1H, q, J_{NH-CH3} = 4.6, 2-NH), 2.91 (3H, d, J_{CH3-NH} = 4.6, 6-NH-**CH_3**); ^{13}C NMR (213.8 MHz, DMSO-d_6) Rotamer CA: 165.9 (C4), 163.4 (C2), 151.1 (C6), 136.9 (C5), 28.1 (C2-NH-**CH_3**), 25.9 (C6-NH-**CH_3**), Rotamer CB: 163.3 (C6), 163.1 (C2), 150.9 (C4), 137.6 (C5), 27.9 (C2-NH-**CH_3**), 27.3 (C6-NH-**CH_3**), Rotamer DA: 165.3 (C4), 163.1 (C2), 150.8 (C6), 137.0 (C5), 27.9 (C2-NH-**CH_3**), 25.7 (C6-NH-**CH_3**), Rotamer DB: 163.2 (C2), 162.9 (C6), 150.8 (C4), 137.6 (C5), 28.1 (C2-NH-**CH_3**), 27.4 (C6-NH-**CH_3**); ESI MS, m/z (%) 183.1 [M + H]$^+$; HRMS (ESI) calcd for $C_6H_{11}N_6O$ [M + H]$^+$ 183.0988, found 183.0990.

*2-Methoxy-N^6-methyl-5-nitrosopyrimidin-4,6-diamine (**5c**).* Compound **5c** (20 mg, 22%) was obtained as a violet solid with mp 215−217 °C. ^{1}H NMR (500.0 MHz, DMSO-d_6) Rotamer A: 11.25 (1H, q, J_{NH-CH3} = 4.9, 6-NH), 8.88 and 8.05 (2 × 1H, 2*s*, 4-NH_2), 3.87 (3H, s, O−CH_3), 2.89 (3H, d, J_{CH3-NH} = 4.9, NH−CH_3), Rotamer B: 10.40 (1H, s, 4-NH^A), 9.40 (1H, q, J_{NH-CH3} = 4.7, 6-NH), 8.51 (1H, s, 4-NH^B), 3.87 (3H, s, O−CH_3), 3.00 (3H, d, J_{CH3-NH} = 4.7, NH−CH_3); ^{13}C NMR (125.7 MHz, DMSO-d_6) Rotamer A: 167.9 (C2), 165.1 (C4), 150.2 (C6), 138.4 (C5), 54.8 (O−CH_3), 26.4 (NH−CH_3), Rotamer B: 167.6 and 167.5 (C2 and C6), 150.1 (C4), 139.1 (C5), 54.8 (O−CH_3), 27.8 (NH−CH_3); ESI MS, m/z (%) 184.2 [M + H]$^+$; HRMS (ESI) calcd for $C_6H_{10}N_5O_2$ [M + H]$^+$ 184.0829, found 184.0829.

*N^6-Methyl-2-(methylthio)pyrimidine-4,6-diamine (**11**).* Compound **8** (800 mg, 4.6 mmol) was treated with methylamine (157 mg, 5.1 mmol, 33% ethanolic solution) in *i*PrOH (30 mL) under MW conditions (180 °C, 1 h). Water (50 mL) was added and the obtained solution was extracted with EtOAc (3 × 30 mL). Organic layers were collected, dried over $MgSO_4$ and filtered. Solvents were evaporated under vacuum. Silica gel column chromatography (10% MeOH in $CHCl_3$) gave **11** (390 mg, 50%) as a white solid with mp 144−146 °C. ^{1}H NMR (401.0 MHz, DMSO-d_6) 6.50 (1H, q, J_{NH-CH3} = 4.6, NH), 6.09 (2H, s, NH_2), 5.07 (1H, s, H5), 2.66 (3H, d, J_{CH3-NH} = 4.6, NH-**CH_3**), 2.34 (3H, s, S-CH_3); ^{13}C NMR (100.8 MHz, DMSO-d_6) 168.7 (C2), 163.4 (C6), 163.2 (C4), 77.6 (C5), 27.6 (NH−CH_3), 13.1 (S-CH_3); ESI MS, m/z (%) 171.1 [M + H]$^+$; HRMS (ESI) calcd for $C_6H_{11}N_4S$ [M + H]$^+$ 171.0704, found 171.0705.

*N^6-Methyl-2-(methylthio)-5-nitrosopyrimidin-4,6-diamine (**5d**).* Treatment of **11** (100 mg, 0.6 mmol) with IAN (77 mg, 0.66 mmol) by general method A gave **5d** (110 mg, 92%) as a green solid with mp 233−236 °C. ^{1}H NMR (500.0 MHz, DMSO-d_6) Rotamer A: 11.24 (1H, q, J_{NH-CH3} = 4.9, 6-NH), 8.94 and 8.01 (2 × 1H, 2*s*, 4-NH_2), 2.91 (3H, d, J_{CH3-NH} = 4.9, NH-**CH_3**), 2.48 (3H, s, S-CH_3), Rotamer B: 10.31 (1H, s, 4-NH^A), 9.50 (1H, q, J_{NH-CH3} = 4.8, 6-NH), 8.44 (1H, s, 4-NH^B), 3.03 (3H, d, J_{CH3-NH} = 4.8, NH-**CH_3**), 2.50 (3H, s, S-CH_3); ^{13}C NMR (125.7 MHz, DMSO-d_6) Rotamer A: 178.8 (C2), 164.3 (C4), 146.0 (C6), 138.4 (C5), 26.3 (NH−CH_3), 13.9 (S-CH_3), Rotamer B: 178.7 (C2), 161.5 (C6), 145.8 (C4), 139.1 (C5), 27.8 (NH−CH_3), 13.9 (S-CH_3); ESI MS, m/z (%) 200.2 [M + H]$^+$; HRMS (ESI) calcd for $C_6H_{10}N_5OS$ [M + H]$^+$ 200.0600, found 200.0601.

*6-Chloro-2-methylpyrimidin-4-amine (**13**).* Compound **12** (500 mg, 3.1 mmol) was treated with ammonia (2.5 M ethanolic solution) under MW conditions (140 °C, 1 h). Water (100 mL) was added and obtained solution was extracted with EtOAc (3 × 40 mL). Organic layers were collected, dried over $MgSO_4$ and filtered. Solution was evaporated under vacuum. Compound **13** (400 mg, 90%) was obtained as a white solid with mp 188−190 °C. ^{1}H NMR (500.0 MHz, DMSO-d_6) 7.12 (2H, s, 4-NH_2), 6.26 (1H, s, 5-H), 2.28 (3H, s, 2-CH_3); ^{13}C NMR (125.7 MHz, DMSO-d_6) 167.8 (C2), 165.1 (C4), 158.0 (C6), 99.9 (C5), 25.3 (2-CH_3); ESI MS, m/z (%) 144.0 [M + H]$^+$; HRMS (ESI) calcd for $C_5H_7N_3Cl$ [M + H]$^+$ 144.0323, found 144.0323.

*2-Methyl-N^6-methylpyrimidin-4,6-diamine (**14**).* Mixture of **13** (400 mg, 2.8 mmol) and methylamine (95.5 mg, 3.1 mmol, 33% ethanolic solution) in *i*PrOH (30 mL) was treated under MW conditions (160 °C, 3 h). Solvents were evaporated under vacuum. The silica gel column chromatography (10% MeOH in $CHCl_3$) gave **14** (270 mg, 70%) as a white solid with mp 215−230 °C. ^{1}H NMR (500.0 MHz, DMSO-d_6) 6.98 (1H, s, 6-NH), 6.51 (2H, s, 4-NH_2), 5.24 (1H, s, H5), 2.68 (3H, d, J_{NH-CH3} = 4.8, NH−CH_3), 2.19 (3H, s, 2-CH_3); ^{13}C NMR (125.7 MHz, DMSO-d_6) 163.1 (C2), 162.9 (C6), 161.3 (C4), 78.0 (C5), 27.8 (NH−CH_3), 24.1 (2-CH_3); ESI MS, m/z (%) 139.1 [M + H]$^+$; HRMS (ESI) calcd for $C_6H_{11}N_4$ [M + H]$^+$ 139.0978, found 139.0979.

DOI: 10.1021/acs.joc.6b00446
J. Org. Chem. 2016, 81, 3780−3789

*2-Methyl-N⁶-methyl-5-nitrosopyrimidin-4,6-diamine (**5e**).* Treatment of **14** (100 mg, 0.7 mmol) with IAN (90 mg, 0.77 mmol) by general method A gave **5e** (40 mg, 34%) as a green solid with mp 198−199 °C. ^{1}H NMR (500.0 MHz, DMSO-d_6) Rotamer A: 11.13 (1H, q, J_{NH-CH3} = 5.1, **NH**-CH_3), 8.94 and 7.97 (2 × 1H, 2*s*, 4-NH_2), 2.89 (3H, d, J_{CH3-NH} = 5.1, NH-**CH_3**), 2.24 (3H, s, 2-CH_3), Rotamer B: 10.21 (1H, s, 4-NH^A), 9.43 (1H, q, J_{NH-CH3} = 4.8, **NH**-CH_3), 8.40 (1H, s, 4-NH^B), 3.02 (3H, d, J_{CH3-NH} = 4.8, NH-**CH_3**), 2.24 (3H, s, 2-CH_3); ^{13}C NMR (125.7 MHz, DMSO-d_6) Rotamer A: 174.9 (C2), 166.0 (C4), 146.8 (C6), 138.9 (C5), 27.0 (2-CH_3), 26.3 (NH−CH_3), Rotamer B: 174.7 (C2), 163.2 (C6), 146.3 (C4), 139.7 (C5), 27.8 (NH−CH_3), 27.1 (2-CH_3); ESI MS, *m*/*z* (%) 168.1 $[M + H]^+$; HRMS (ESI) calcd for $C_6H_{10}N_5O$ $[M + H]^+$ 168.0879, found 168.0879.

*N⁶-Methylpyrimidin-4,6-dimamine (**16**).* A solution of **15** (700 mg, 5.4 mmol) and methylamine (184 mg, 6 mmol, 33% ethanolic solution) in *i*PrOH (20 mL) was heated under MW conditions (180 °C, 1 h). The solvent was evaporated under vacuum. The silica gel column chromatography (20% MeOH in $CHCl_3$) gave **16** (335 mg, 54%) as a yellowish solid with mp 215−230 °C. ^{1}H NMR (401.0 MHz, DMSO-d_6) 7.84 (1H, s, H2), 6.50 (1H, q, J_{NH-CH3} = 4.9, NH), 6.07 (2H, s, NH_2), 5.31 (1H, s, H5), 2.66 (3H, d, J_{CH3-NH} = 4.9, NH-**CH_3**); ^{13}C NMR (100.8 MHz, DMSO-d_6) 163.5 (C6), 163.3 (C4), 157.6 (C2), 81.1 (C5), 27.6 (NH−CH_3); ESI MS, *m*/*z* (%) 125.1 $[M + H]^+$; HRMS (ESI) calcd for $C_5H_9N_4$ $[M + H]^+$ 125.0827, found 125.0825.

*N⁶-Methyl-5-nitrosopyrimidin-4,6-diamine (**5f**).* HCl (35% aqueous solution) was added dropwise to the solution of compound **16** (100 mg, 0.8 mmol) in water (10 mL) until the solution became clear. The reaction mixture was stirred at 0−5 °C for 5 min and a solution of sodium nitrite (76 mg, 1.1 mmol) in water (5 mL) was added dropwise. Stirring was continued at room temperature for 1 h. The colorless solution was neutralized with aqueous $NaHCO_3$ solution and green solid precipitated. Filtration afforded **5f** (40 mg, 33%) as a green solid with mp 198−200 °C. ^{1}H NMR (500.0 MHz, DMSO-d_6) Rotamer A: 11.12 (1H, q, J_{NH-CH3} = 5.1, 6-NH), 9.14 and 8.12 (2 × 1H, 2 × bs, 4-NH_2), 8.02 (1H, s, H2), 2.90 (3H, d, J_{CH3-NH} = 5.1, CH_3), Rotamer B: 10.25 (1H, bs, 4-NH^A), 9.62 (1H, bs, 6-NH), 8.55 (1H, bs, 4-NH^B), 8.02 (1H, s, H2), 3.04 (3H, d, J_{CH3-NH} = 3.6, CH_3); ^{13}C NMR (125.7 MHz, DMSO-d_6) Rotamer A: 166.1 (C4), 164.9 (C2), 146.2 (C6), 140.2 (C5), 26.5 (NH−CH_3), Rotamer B: 164.8 (C2), 163.3 (C6), 145.7 (C4), 140.9 (C5), 27.9 (NH−CH_3); ESI MS, *m*/*z* (%) 154.2 $[M + H]^+$; HRMS (ESI) calcd for $C_5H_8N_5O$ $[M + H]^+$ 154.0723, found 154.0724.

■ ASSOCIATED CONTENT

Supporting Information

The Supporting Information is available free of charge on the ACS Publications website at DOI: 10.1021/acs.joc.6b00446.

Additional NMR, UV−vis and EPR spectra, calculated NMR and EPR parameters, ^{1}H and ^{13}C spectra of newly prepared compounds, Cartesian coordinates of transition-state structures. (PDF)

■ AUTHOR INFORMATION

Corresponding Authors

*E-mail: janeba@uochb.cas.cz.
*E-mail: dracinsky@uochb.cas.cz.

Notes

The authors declare no competing financial interest.

■ ACKNOWLEDGMENTS

The work has been supported by the Czech Science Foundation (grant no. 15-11223S).

■ REFERENCES

(1) Vančik, H. *Aromatic C-Nitroso Compounds*; Springer: New York, 2013.
(2) Carosso, S.; Miller, M. J. *Org. Biomol. Chem.* **2014**, *12*, 7445−7468.
(3) Yamamoto, H.; Momiyama, N. *Chem. Commun.* **2005**, 3514−3525.
(4) Beaudoin, D.; Wuest, J. D. *Chem. Rev.* **2016**, *116*, 258−286.
(5) Liu, L.; Wagner, C. R.; Hanna, P. E. *Chem. Res. Toxicol.* **2009**, *22*, 1962−1974.
(6) Trefzer, C.; Rengifo-Gonzalez, M.; Hinner, M. J.; Schneider, P.; Makarov, V.; Cole, S. T.; Johnsson, K. *J. Am. Chem. Soc.* **2010**, *132*, 13663−13665.
(7) Peng, L. J.; Turesky, R. J. *J. Proteomics* **2014**, *103*, 267−278.
(8) Gunther, M. R. *Free Radical Biol. Med.* **2004**, *36*, 1345−1354.
(9) Hawkins, C. L.; Davies, M. J. *Biochim. Biophys. Acta, Gen. Subj.* **2014**, *1840*, 708−721.
(10) Procházková, E.; Čechová, L.; Janeba, Z.; Dračínský, M. *J. Org. Chem.* **2013**, *78*, 10121−10133.
(11) Susvilo, I.; Brukstus, A.; Tumkevicius, S. *Tetrahedron Lett.* **2005**, *46*, 1841−1844.
(12) Marchal, A.; Nogueras, M.; Sanchez, A.; Low, J. N.; Naesens, L.; De Clercq, E.; Melguizo, M. *Eur. J. Org. Chem.* **2010**, *2010*, 3823−3830.
(13) Olivella, M.; Marchal, A.; Nogueras, M.; Melguizo, M.; Lima, B.; Tapia, A.; Feresin, G. E.; Parravicini, O.; Giannini, F.; Andujar, S. A.; Cobo, J.; Enriz, R. D. *Arch. Pharm.* **2015**, *348*, 68−80.
(14) Čechová, L.; Procházková, E.; Císařová, I.; Dračínský, M.; Janeba, Z. *Chem. Commun.* **2014**, *50*, 14892−14895.
(15) Kuhn, B.; Mohr, P.; Stahl, M. *J. Med. Chem.* **2010**, *53*, 2601−2611.
(16) Gilli, G.; Bellucci, F.; Ferretti, V.; Bertolasi, V. *J. Am. Chem. Soc.* **1989**, *111*, 1023−1028.
(17) Gilli, P.; Bertolasi, V.; Ferretti, V.; Gilli, G. *J. Am. Chem. Soc.* **2000**, *122*, 10405−10417.
(18) Dračínský, M.; Čechová, L.; Hodgkinson, P.; Procházková, E.; Janeba, Z. *Chem. Commun.* **2015**, *51*, 13986−13989.
(19) Bureš, F. *RSC Adv.* **2014**, *4*, 58826−58851.
(20) de la Torre, G.; Vazquez, P.; Agullo-Lopez, F.; Torres, T. *Chem. Rev.* **2004**, *104*, 3723−3750.
(21) Abbotto, A.; Beverina, L.; Bozio, R.; Bradamante, S.; Ferrante, C.; Pagani, G. A.; Signorini, R. *Adv. Mater.* **2000**, *12*, 1963−1967.
(22) Meier, H. *Angew. Chem., Int. Ed.* **2005**, *44*, 2482−2506.
(23) He, G. S.; Tan, L. S.; Zheng, Q.; Prasad, P. N. *Chem. Rev.* **2008**, *108*, 1245−1330.
(24) Imahori, H.; Umeyama, T.; Ito, S. *Acc. Chem. Res.* **2009**, *42*, 1809−1818.
(25) Clifford, J. N.; Martinez-Ferrero, E.; Viterisi, A.; Palomares, E. *Chem. Soc. Rev.* **2011**, *40*, 1635−1646.
(26) Wu, Y. Z.; Zhu, W. H. *Chem. Soc. Rev.* **2013**, *42*, 2039−2058.
(27) Sullivan, P. A.; Dalton, L. R. *Acc. Chem. Res.* **2010**, *43*, 10−18.
(28) Chen, F. K.; Zhang, J.; Wan, X. H. *Chem. - Eur. J.* **2012**, *18*, 4558−4567.
(29) Wu, Y. L.; Tancini, F.; Schweizer, W. B.; Paunescu, D.; Boudon, C.; Gisselbrecht, J. P.; Jarowski, P. D.; Dalcanale, E.; Diederich, F. *Chem. - Asian J.* **2012**, *7*, 1185−1190.
(30) Shao, P.; Huang, B.; Chen, L. Q.; Liu, Z. J.; Qin, J. G.; Gong, H. M.; Ding, S.; Wang, Q. Q. *J. Mater. Chem.* **2005**, *15*, 4502−4506.
(31) Abbotto, A.; Beverina, L.; Bozio, R.; Facchetti, A.; Ferrante, C.; Pagani, G. A.; Pedron, D.; Signorini, R. *Org. Lett.* **2002**, *4*, 1495−1498.
(32) Zheng, S. J.; Beverina, L.; Barlow, S.; Zojer, E.; Fu, J.; Padilha, L. A.; Fink, C.; Kwon, O.; Yi, Y. P.; Shuai, Z. G.; Van Stryland, E. W.; Hagan, D. J.; Bredas, J. L.; Marder, S. R. *Chem. Commun.* **2007**, 1372−1374.
(33) Kato, S.; Matsumoto, T.; Shigeiwa, M.; Gorohmaru, H.; Maeda, S.; Ishi-i, T.; Mataka, S. *Chem. - Eur. J.* **2006**, *12*, 2303−2317.
(34) Hrobárikova, V.; Hrobárik, P.; Gajdoš, P.; Fitilis, I.; Fakis, M.; Persephonis, P.; Zahradník, P. *J. Org. Chem.* **2010**, *75*, 3053−3068.

DOI: 10.1021/acs.joc.6b00446
J. Org. Chem. 2016, 81, 3780−3789

(35) Kleinpeter, E.; Koch, A. *J. Phys. Chem. A* **2009**, *113*, 10852−10857.
(36) Kleinpeter, E.; Klod, S.; Rudorf, W. D. *J. Org. Chem.* **2004**, *69*, 4317−4329.
(37) Dračínský, M.; Bouř, P. *J. Chem. Theory Comput.* **2010**, *6*, 288−299.
(38) Bard, A. J.; Faulkner, L. R. *Electrochemical Methods: Fundamentals and Applications*, 2nd ed.; Wiley & Sons: New York, 2001.
(39) Gronchi, G.; Tordo, P. *Res. Chem. Intermed.* **1993**, *19*, 733−753.
(40) Stoll, S.; Schweiger, A. *J. Magn. Reson.* **2006**, *178*, 42−55.
(41) http://www.easyspin.org/.
(42) Becke, A. D. *J. Chem. Phys.* **1993**, *98*, 5648−5652.
(43) Lee, C. T.; Yang, W. T.; Parr, R. G. *Phys. Rev. B: Condens. Matter Mater. Phys.* **1988**, *37*, 785−789.
(44) Barone, V.; Cossi, M. *J. Phys. Chem. A* **1998**, *102*, 1995−2001.
(45) Cossi, M.; Rega, N.; Scalmani, G.; Barone, V. *J. Comput. Chem.* **2003**, *24*, 669−681.
(46) Frisch, M. J.; Trucks, G. W.; Schlegel, H. B.; Scuseria, G. E.; Robb, M. A.; Cheeseman, J. R.; Scalmani, G.; Barone, V.; Mennucci, B.; Petersson, G. A.; Nakatsuji, H.; Caricato, X.; Li, X.; Hratchian, H. P.; Izmaylov, A. F.; Bloino, J.; Zheng, G.; Sonnenberg, J. L.; Hada, M.; Ehara, M.; Toyota, K.; Fukuda, R.; Hasegawa, J.; Ishida, M.; Nakajima, T.; Honda, Y.; Kitao, O.; Nakai, H.; Vreven, T.; Montgomery, J. A.; Peralta, J. E.; Ogliaro, F.; Bearpark, M.; Heyd, J. J.; Brothers, E.; Kudin, K. N.; Staroverov, V. N.; Kobayashi, R.; Normand, J.; Raghavachari, K.; Rendell, A.; Burant, J. C.; Iyengar, S. S.; Tomasi, J.; Cossi, M.; Rega, N.; Millam, J. M.; Klene, M.; Knox, J. E.; Cross, J. B.; Bakken, V.; Adamo, C.; Jaramillo, J.; Gomperts, R.; Stratmann, R. E.; Yazyev, O.; Austin, A. J.; Cammi, R.; Pomelli, C.; Ochterski, J. W.; Martin, R. L.; Morokuma, K.; Zakrzewski, V. G.; Voth, G. A.; Salvador, P.; Dannenberg, J. J.; Dapprich, S.; Daniels, A. D.; Farkas, O.; Foresman, J. B.; Ortiz, J. V.; Cioslowski, J.; Fox, D. J. *Gaussian 09*, Revision A.02; Gaussian, Inc.: Wallingford, CT, 2009.
(47) Peng, C.; Ayala, P. Y.; Schlegel, H. B.; Frisch, M. J. *J. Comput. Chem.* **1996**, *17*, 49−56.
(48) Peng, C.; Schlegel, H. B. *Isr. J. Chem.* **1994**, *33*, 449−454.
(49) Bauernschmitt, R.; Ahlrichs, R. *Chem. Phys. Lett.* **1996**, *256*, 454−464.
(50) Barone, V. *Recent Advances in Density Functional Methods, Part I*, 1st ed.; World Scientific Publ. Co.: Singapore, 1996.
(51) Wang, T.; Brudvig, G. W.; Batista, V. S. *J. Chem. Theory Comput.* **2010**, *6*, 2395−2401.
(52) Zhao, Y.; Truhlar, D. G. *J. Chem. Phys.* **2006**, *125*, 194101−194119.
(53) Kendall, R. A.; Dunning, T. H.; Harrison, R. J. *J. Chem. Phys.* **1992**, *96*, 6796−6806.
(54) Humphrey, W.; Dalke, A.; Schulten, K. *J. Mol. Graphics* **1996**, *14*, 33−38.
(55) http://www.ks.uiuc.edu/Research/vmd/.

DOI: 10.1021/acs.joc.6b00446
J. Org. Chem. 2016, 81, 3780−3789